Dynamics of Miscible Polymer Blends: Predicting the Dielectric Response

Sergei Shenogin,[†] Rama Kant,[‡] Ralph H. Colby,[§] and Sanat K. Kumar*,[⊥]

Rensselaer Nanotechnology Center, Rensselaer Polytechnic Institute, Troy, New York 12180; Department of Chemical Engineering, Rensselaer Polytechnic Institute, Troy, New York 12180; Department of Materials Science and Engineering, The Pennsylvania State University, University Park, Pennsylvania 16802; and Department of Chemical Engineering, Columbia University, New York, New York 10027

Received February 28, 2007; Revised Manuscript Received May 7, 2007

ABSTRACT: We present a predictive model for the dynamics of miscible polymer blends by assuming that local composition variations determine segmental dynamics. We then properly incorporate the distributions of intrachain ("self-concentration") and interchain ("concentration fluctuations") contributions to the compositions surrounding a polymer segment. In a manner similar to our past work we then derive the distribution of relaxation times for both components. These distributions depend explicitly on the size of the volume in which fluctuations are sampled by the test segment. We find by fitting our model to an extensive body of data on various miscible blends (PI/PVE, PBO/PVE, PVME/PS, and PVME/P2ClS) that an essentially composition-independent value of the correlation volume reproduces all available segmental relaxation data at temperatures above the glass transition of the low-T_g component. We have shown that the apparent temperature dependence of the size of the correlation volume is very weak at all temperatures above the T_g of the low-T_g component. The size of the correlation volume is found to be comparable to the Kuhn segment length of the chains. While our approach thus resembles the model of Lodge and McLeish, it is important to emphasize that we include the distributions of compositions experienced by a test segment instead of invoking a mean field. The appropriate choice of the size of the correlation volume and proper incorporation of concentration fluctuations are vital to simultaneously model the peak segmental time and the width of the relaxation time spectra. By comparing PI/PVE with PBO/PVE and comparing PVME/PS with PVME/P2ClS, we show that the size of the correlation volume is apparently a polymer-chain-specific property that does not depend on the blend composition and blend partner.

1. Introduction

The viscoelastic properties of miscible polymer blends have been the focus of extensive research in the past 15 years. This work is inspired by the fact that, although the blends are thermodynamically miscible, and hence molecularly mixed, often the component dynamics are heterogeneous. Dynamic heterogeneity is most apparent when the temperature dependence of each component's *mean* segmental relaxation time is different. The empirical time−temperature superposition (tTS) principle[1] then fails dramatically, as in the case of the poly(ethylene oxide) (PEO)/poly(methyl methacrylate) (PMMA) blend.[2−4] From an applications standpoint, thermorheological complexity creates particular difficulties since it becomes hard to formulate broadly based "mixing" rules to predict blend dynamics and hence processability.

Experimentally, thermorheological complexity has only been reported for miscible blends with weak interactions, where the two components have very different glass transition temperatures.[5−12] For systems with $\Delta T_g = |T_{g1} - T_{g2}| < 20$ K, tTS appears to hold.[13−15] For systems with 20 K $< \Delta T_g <$ 70 K, the relaxation times have somewhat different temperature dependences and the differences systematically increase as ΔT_g increases.[16] For larger dynamic asymmetries ($\Delta T_g > 100$ K) these trends become even more accentuated. However, as shown in NMR experiments by Kornfield and co-workers,[7,8] each component's segmental relaxation time distribution remains unimodal but is substantially broadened compared to the pure components. The relaxation time of each component can be apparently well fit by log−normal distributions with modified WLF parameters and glass transition temperatures.

These results appear to be relatively insensitive to system thermodynamics, in that the dynamic behavior does not change dramatically if one approaches the critical point for phase separation. This is understood because weakly interacting polymer mixtures have very small free energies of mixing, with weak temperature dependences owing to the entropy of mixing being related to the inverse of chain length. This makes concentration fluctuations in weakly interacting polymer blends persist hundreds of degrees from the critical point. However, thermodynamics is important when one considers strongly miscible systems where concentration fluctuations are suppressed.[5] While the consensus at this time is that local concentration variations, created by concentration fluctuations (driven by the thermodynamics of the blends) and by chain connectivity effects (i.e., that a certain fraction of monomers in the correlation volume are intramolecular contacts) are responsible for these unusual experimental results, the relative importance of these effects and the relevant volumes over which these effects need to be considered, remain unresolved at this time. In particular:

* To whom correspondence should be addressed. E-mail: sk2794@columbia.edu.
[†] Rensselaer Nanotechnology Center, Rensselaer Polytechnic Institute.
[‡] Department of Chemical Engineering, Rensselaer Polytechnic Institute.
[§] The Pennsylvania State University.
[⊥] Columbia University.

10.1021/ma070503q CCC: $37.00
Published on Web 07/07/2007

1. Zetsche and Fischer[17,18] considered the role of concentration fluctuations on segmental dynamics. By fitting their model to data on the miscible poly(vinyl methyl ether)/polystyrene blend, they concluded that the correlation volume size was dependent on the mean blend composition and temperature. The temperature dependence was assumed to be described by the Donth form,[19] suggesting that the correlation volume is the cooperative volume, which diverges at the Vogel temperature of that blend component. While this approach reproduces the broadening of the blend glass transition as a function of temperature, it fails to lead to the presence of two microenvironments with distinctly different mobilities for the two components regardless of T_g. Further, the size of the correlation volume has a strong temperature dependence and becomes much larger than the Kuhn length (~10 nm at T_g).

2. In an attempt to reproduce the breakdown of tTS, Kornfield et al.[7] included intramolecular connectivity effects, which skew the mean composition experienced by a chosen A polymer segment toward compositions richer in A. Composition fluctuations were incorporated using Bernoulli statistics, i.e., by assuming that segments are distributed at random. Thus, the thermodynamics of these systems are not considered in the Kornfield approach. These workers found that a temperature-independent cooperative volume with lateral size of ~5 nm was sufficient to simultaneously capture the mean values of the relaxation times and the widths of the distributions of relaxation times in a qualitative fashion.

3. Lodge and McLeish[21] used the same ideas as Kornfield but with two differences. First, they suggested that the lateral sizes of the cooperative volumes are small, equal to the Kuhn length of the chains. Second, they did not consider concentration fluctuation effects. These workers thus developed a model which only considered chain connectivity effects. Since concentration fluctuations affect both the distributions and peak segmental times, especially close to the blend T_g,[22,23] this model does not describe distributions and only qualitatively describes the temperature dependence of peak segmental times far above T_g. This is reflected in the wide range of self-compositions required to understand blend dynamics with this simplest of models, as temperature and blend partner are varied.[24]

4. Kumar and co-workers[25,26] approximately accounted for concentration fluctuations and intramolecular connectivity effects using the ideas of Zetsche and Fischer and Kornfield et al., respectively. As in the work of Zetsche and Fischer,[17] this model needed to utilize large length scales for the correlation volume to obtain agreement with experiments. However, both the variation of the mean relaxation time of each species and the widths of the distributions could be simultaneously reproduced.

5. Colby and Lipson[27] used a lattice model to demonstrate that with a small correlation volume (of order 1 nm) the segmental dynamics of PI and PVE could be modeled reasonably for various temperatures and blend compositions, using Bernoullian statistics and accounting for connectivity of all chains in the fixed correlation volume. An open question is whether such ideas can still be used very close to T_g and for all compositions and blend partners.

Here we improve our earlier theory[22] by explicitly incorporating a better understanding of both intermolecular and intramolecular concentration distributions. This improved model is then fit in a detailed manner to all available dielectric data for four polymer blends with various compositions. We show that the size of the correlation volume for segmental dynamics of each component, that quantitatively describes the distributions of segmental dynamics, is composition-independent and very weakly temperature-dependent, even close to the T_g of the blend. Further, since the size scales of the correlation volume of a component do not depend on blend partner, we suggest that the previous results of Ediger, who had suggested that the mean-field value of the self-concentration (obtained by fitting the Lodge−McLeish model) depended on the blend partner, must be a consequence of the fact that these workers ignored concentration fluctuations. We thus stress that the inclusion of concentration fluctuations and chain connectivity effects are both necessary for a quantitative understanding of all aspects of miscible blend dynamics.

2. Model Description

We postulate that segmental dynamics are controlled by the local composition within a sphere of radius R_c centered at a given segment. Following Kornfield et al.,[7] the effective concentration of A monomers in the vicinity of an A monomer can be written in terms of the intramolecular, or self-concentration (ϕ^A_{self}), and the intermolecular concentration ϕ^A as

$$\phi^A_{eff} = \phi^A_{self} + (1 - \phi^A_{self})\phi^A \quad (1)$$

A similar equation can be written for the B species. Following Zetsche and Fischer,[17] we assume that the variation of local composition ϕ^A_{eff} is responsible for broadening of the relaxation spectra. To find the distribution of the relaxation times, we need (1) to find the distribution of effective concentration of A monomers in the vicinity of an A monomer and (2) to define the connection between local composition and local relaxation time.

1. Distribution of Effective Compositions. For small correlation volumes ($R_c < b$, where b is the Kuhn segment length), the intramolecular concentration ϕ_{self} is constant, since the chain is inflexible at this scale:[21]

$$\phi^A_{self} = \frac{3}{2\pi}\frac{v_A}{b_A R_c^2}, \quad R_c < b_A \quad (2)$$

where v_A is the volume occupied by a single A monomer. Therefore, the mean effective volume fraction of A segments in the correlation volume surrounding an A monomer can be found from eq 1 as

$$\bar{\phi}^A_{eff} = \phi^A_{self} + (1 - \phi^A_{self})\Phi_A \quad (3)$$

where Φ_A is the mean blend composition.

We now develop the probability distribution function (PDF) for ϕ^A_{eff} around the mean value $\bar{\phi}^A_{eff}$ by constructing the PDF for intermolecular concentration ϕ^A.

The distribution of intermolecular concentration in an arbitrary chosen volume of a given size (i.e., not centered around a monomer of a given type) assumes a standard Gaussian form (for component A, with analogous expression for component B):

$$p(\phi^A) = \frac{1}{\sqrt{2\pi\langle\delta\phi^2\rangle}}\exp\left\{-\frac{(\phi^A - \Phi_A)^2}{2\langle\delta\phi^2\rangle}\right\} \quad (4)$$

where $\langle\delta\phi^2\rangle$ is the mean-squared concentration fluctuation. If the blend is incompressible, the parameter $\langle\delta\phi^2\rangle$ must be equal for both species (A or B). From eqs 1 and 3, the PDF for ϕ^A_{eff} will then take the form

$$p(\phi_{\mathrm{eff}}^{\mathrm{A}}) = \frac{1}{\sqrt{2\pi\langle\delta\phi_{\mathrm{eff,A}}{}^2\rangle}} \exp\left\{-\frac{(\phi_{\mathrm{eff}}^{\mathrm{A}} - \bar{\phi}_{\mathrm{eff}}^{\mathrm{A}})^2}{2\langle\delta\phi_{\mathrm{eff,A}}{}^2\rangle}\right\} \quad (5)$$

with the mean-squared concentration fluctuation[22]

$$\langle\delta\phi_{\mathrm{eff,A}}{}^2\rangle = (1 - \phi_{\mathrm{self}}^{\mathrm{A}})^2\langle\delta\phi^2\rangle \quad (6)$$

Because the valid argument range for eq 5 is $\phi_{\mathrm{self}}^{\mathrm{A}} < \phi_{\mathrm{eff}}^{\mathrm{A}} < 1$, the PDF for $\phi_{\mathrm{eff}}^{\mathrm{A}}$ (eq 5) was renormalized within these boundaries. In the presence of "cutoff" boundaries the shape of equilibrium PDF can differ from eq 5; however, we will use the Gaussian form as an approximation, strictly valid for narrow distributions and nondilute compositions, $\sqrt{\langle\delta\phi_{\mathrm{eff}}{}^2\rangle} \ll \bar{\phi}_{\mathrm{eff}} \ll 1 - \sqrt{\langle\delta\phi_{\mathrm{eff}}{}^2\rangle}$.

Following the formalism implemented by Song and Roe[28] and by Zetsche and Fischer,[17] we derive the expression for the mean-squared concentration fluctuation in an incompressible binary blend:

$$\langle\delta\phi_{\mathrm{A}}{}^2\rangle = \langle\delta\phi_{\mathrm{B}}{}^2\rangle = \langle\delta\phi^2\rangle = \frac{\sqrt{\upsilon_{\mathrm{A}}\upsilon_{\mathrm{B}}}}{4\pi^2}\int_0^\infty S(q)[qF(q)]^2\,\mathrm{d}q \quad (7)$$

where υ_{A} and υ_{B} are the monomer volumes of species A and B, $S(q)$ is the static structure factor, q is the wavevector, and $F(q)$ is the form factor of the correlation volume. Unlike the formula given by Zetsche and Fischer,[17,29] eq 7 predicts the same mean-squared concentration fluctuations for A and B components in arbitrary chosen volumes of the same size, as it should for an incompressible blend.

The form factor of the correlation volume having the shape of a sphere with radius R_{c} is calculated as follows:[30]

$$F(q) = \frac{3[\sin(qR_{\mathrm{c}}) - qR_{\mathrm{c}}\cos(qR_{\mathrm{c}})]}{(qR_{\mathrm{c}})^3} \quad (8)$$

For polymeric blends, the volumes υ_{A} and υ_{B} occupied by single segments of species A and B can be found in terms of packing lengths l_{pA} and l_{pB} and Kuhn lengths b_{A} and b_{B}:[31]

$$\upsilon_{\mathrm{A}} = l_{\mathrm{pA}}b_{\mathrm{A}}{}^2, \quad \upsilon_{\mathrm{B}} = l_{\mathrm{pB}}b_{\mathrm{B}}{}^2 \quad (9)$$

The random phase approximation (RPA) for a Gaussian coil is employed to calculate $S(q)$:[32]

$$\frac{1}{S(q)} = \frac{1}{\Phi_{\mathrm{A}}N_{\mathrm{A}}g_{\mathrm{D}}^{\mathrm{A}}(q)} + \frac{1}{\Phi_{\mathrm{B}}N_{\mathrm{B}}g_{\mathrm{D}}^{\mathrm{B}}(q)} - 2\chi(T) \quad (10)$$

where N_{A} and N_{B} are the degrees of polymerization for species A and B. The Flory interaction parameter χ is temperature dependent and can be approximated as $\chi(T) = 7.42 \times 10^{-3} - 3.22/T$ for PI/PVE blends[33] and $\chi(T) = 0.018 - 7.74/T$ for hhPP/PIB blends.[34] However, in all cases studied here this parameter can be ignored ($\chi(T) = 0$) since it did not show any noticeable effect on the calculated relaxation spectra for weakly interacting blends. To facilitate the evaluation of eq 7, we use the following approximation for the Debye function, g_{D}, which is good to within 15% for the whole range of q:[35]

$$g_{\mathrm{D}}(q) = \frac{2}{q^4R_{\mathrm{g}}{}^4}[\mathrm{e}^{-q^2R_{\mathrm{g}}{}^2} + q^2R_{\mathrm{g}}{}^2 - 1] \approx \frac{1}{(1 + q^2R_{\mathrm{g}}{}^2/2)} \quad (11)$$

where $R_{\mathrm{g}}{}^2 = Nb^2/6$ is the radius of gyration of the chain considered. Equation 7 then simplifies to

$$\langle\delta\phi^2\rangle = \frac{3\sqrt{\upsilon_{\mathrm{A}}\upsilon_{\mathrm{B}}}}{8\pi}\frac{S(0)}{R_{\mathrm{c}}{}^3}\left\{1 - \frac{3(1 + \check{R}_{\mathrm{c}})^2}{2\check{R}_{\mathrm{c}}{}^3}\left[\frac{\check{R}_{\mathrm{c}} - 1}{\check{R}_{\mathrm{c}} + 1} + \mathrm{e}^{-2\check{R}_{\mathrm{c}}}\right]\right\} \quad (12)$$

where $\check{R}_{\mathrm{c}} = R_{\mathrm{c}}/\xi$, and ξ is the correlation length for concentration fluctuations:

$$\xi^2 = \frac{S(0)}{12}[b_{\mathrm{A}}{}^2/\Phi_{\mathrm{A}} + b_{\mathrm{B}}{}^2/\Phi_{\mathrm{B}}] \quad (13)$$

The length ξ is of the order of 50−80 Å for PI/PVE and 110−160 Å for PVME/PS blends. For small correlation volumes ($\check{R}_{\mathrm{c}} < 0.3$) eq 12 can be further simplified to

$$\langle\delta\phi^2\rangle = \frac{3\sqrt{\upsilon_{\mathrm{A}}\upsilon_{\mathrm{B}}}}{2\pi R_{\mathrm{c}}}\left[\frac{b_{\mathrm{A}}{}^2}{\Phi_{\mathrm{A}}} + \frac{b_{\mathrm{B}}{}^2}{\Phi_{\mathrm{B}}}\right]^{-1} \quad (14)$$

A few points need to be stressed here. First, note that, in agreement with past simulations,[29] the mean-squared concentration fluctuation decreases with increasing R_{c}—the predicted power law dependence is verified by the simulations in this range of R_{c} values. Second, for the simplest case where the monomers of the two chains are matched in size ($\upsilon_{\mathrm{A}} = \upsilon_{\mathrm{B}}$, $l_{\mathrm{pA}} = l_{\mathrm{pB}}$, and $b_{\mathrm{A}} = b_{\mathrm{B}}$) it follows that $\langle\delta\phi^2\rangle = 3l_{\mathrm{p}}\Phi_{\mathrm{A}}\Phi_{\mathrm{B}}/2\pi R_{\mathrm{c}}$. This result suggests that for most weakly interacting blends with $\langle\delta\phi^2\rangle \cong 0.1$ the correlation radius is controlled by the packing length, with $2l_{\mathrm{p}} \le R_{\mathrm{c}} \le 2.5l_{\mathrm{p}}$ for the composition range 30−70%. Thus, for most blends we expect that the size scale over which dynamics are averaged is small and not directly related to the Kuhn length of the chains in question. The Kuhn length is typically 2−10 times the packing length, and hence numerically similar to $2R_{\mathrm{c}}$, but the packing length appears to play a more relevant role in determining R_{c}. In this context, we also comment briefly on our earlier findings which had suggested that R_{c} was large.[25,26] This erroneous conclusion stemmed from our earlier ad-hoc approximation: $\langle\delta\phi^2\rangle = b^3S(0)/R_{\mathrm{c}}{}^3$. Thus, for large $S(0)$ (∼1000), as may be expected for weakly interacting blends of long chain length polymers, the only means of reducing the $\langle\delta\phi^2\rangle$ to an acceptable value of 0.1 required that the R_{c} values used were $\sim 20b \sim 20$ nm. The use of the more appropriate form, eq 14, obviates this issue and reduces the size of the averaging volume to a physically more acceptable value. Third, and even more surprisingly, it is apparent that the value of χ does not appear in the final expression, eq 14. We ask if this is inconsistent with the idea that strongly miscible blends do not show a breakdown of tTS? The resolution to this stems from the fact that eq 14 is only valid for small values of the reduced size, $\check{R}_{\mathrm{c}} = R_{\mathrm{c}}/\xi$. In the case of strongly interacting blends, we expect ξ to become comparable to R_{c}, and thus the transition from eq 12 to eq 14 is no longer valid. Rather, we need to go back to the full expression, eq 12, where blend thermodynamics then play a critical role. Finally, eq 14, which may be expected to be valid arbitrarily close to the critical point for phase separation, also shows why weakly interacting blends are not affected by system thermodynamics. In these limits the size scale of the averaging volume is so small that all systems show similar concentration fluctuations. While this result is in excellent agreement with the intuitive arguments presented by Lodge and McLeish, in contrast to this previous work, we argue in the companion paper that concentration fluctuations are critical to capturing even the location of the peak relaxation times.

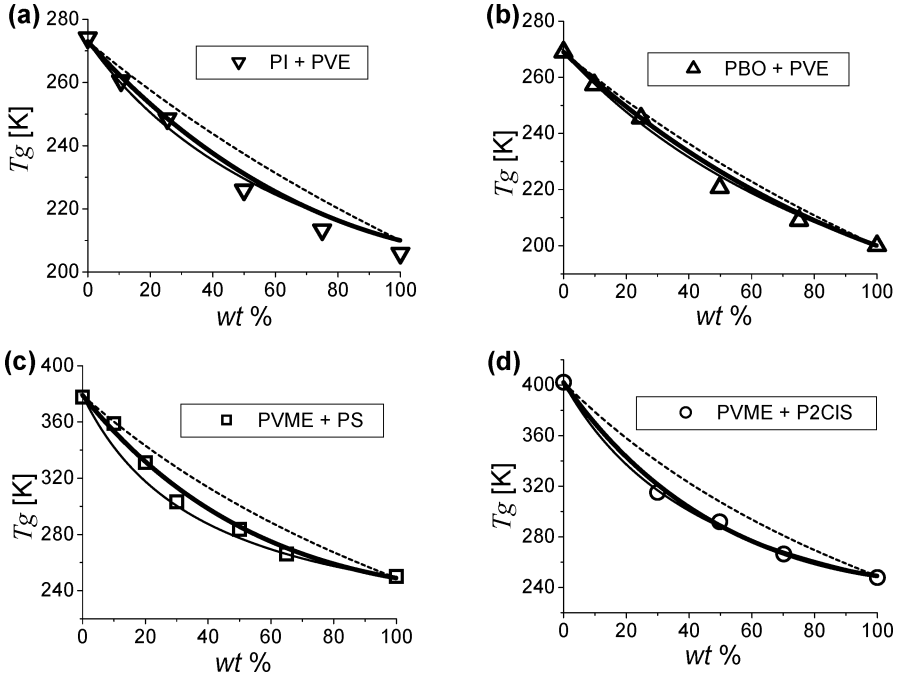

Figure 1. Glass transition temperature of polymer blends plotted vs weight fraction of low-T_g component: DSC data for PI/PVE blends (down triangles),[39] PBO/PVE blends (up triangles),[39] PVME/PS blends (squares),[40] and PVME/P2ClS blends (circles);[40] the results of Fox equation (17b) (dashed lines), the results of DiMarzio equation (17a) with Q as a fitting parameter (thin solid lines), and the predictions of self-concentration model (eq 22) with nonadjustable parameters listed in Table 2 (thick solid lines).

Table 1. Monomer Length Scale Parameters, Best Fit WLF Parameters, and Havriliak−Negami Parameters α and γ Used for Calculation of Dielectric Loss Spectra

blend	components	b (Å)	l_p (Å)	T_g (K)	log(τ_g)	C_1	C_2 (K)	α	γ	refs
1	PI	8.2	3.2	210	0.384	13.2	46.0	0.603	1.03	9, 26
	PVE	14	2.8	273	−0.082	11.8	35.4	0.577	0.595	
2	PBO	8.2	2.5	200	1.303	12.7	41.8	0.620	0.445	39
	PVE-89	14	2.8	269	−0.082	11.8	35.4	0.577	0.595	
3	PVME	13	2.7	249	0.144	12.9	50.3	0.806	0.417	26, 43
	PS	18	3.9	379	1.030	13.3	50.0			
4	PVME	13	2.7	249	0.144	12.9	50.3	0.806	0.417	40
	P2ClS	18	3.9	402	1.030	13.3	50.0	0.820	0.470	

2. Composition Dependence of Relaxation Times and Their Distribution Functions. The probability distribution function (PDF) for the logarithmic segmental relaxation time is related to the PDF for the effective concentration by

$$p_\tau(\ln \tau) = \frac{p(\phi_{\text{eff}})}{\mathrm{d} \ln \tau / \mathrm{d}\phi_{\text{eff}}} \tag{15}$$

The mean logarithmic segmental relaxation time is computed as $\langle \ln\tau \rangle = \int_{-\infty}^{+\infty} p_\tau(\ln\tau)\ \ln\ \tau\ \mathrm{d}\ \ln\tau$, and the width of the distribution of relaxation times is determined by calculating the variance $\sigma^2 = \int_{-\infty}^{+\infty} p_\tau(\ln\ \tau)[\ln\ \tau - \langle \ln\ \tau \rangle]^2\ \mathrm{d}\ \ln\ \tau$.

To convert the distribution of compositions to the distribution of relaxation times, we use the Williams−Landel−Ferry (WLF) equation:[1]

$$\log_{10}\left(\frac{\tau^{\mathrm{A}}(\phi^{\mathrm{A}}_{\text{eff}})}{\tau^{\mathrm{A}}_{\mathrm{g}}}\right) = -\frac{C_1^{\mathrm{A}}(T - T_{\mathrm{g}}^{\mathrm{A}}(\phi^{\mathrm{A}}_{\text{eff}}))}{C_2^{\mathrm{A}}(\phi^{\mathrm{A}}_{\text{eff}}) + T - T_{\mathrm{g}}^{\mathrm{A}}(\phi^{\mathrm{A}}_{\text{eff}})} \tag{16}$$

The composition dependence of glass transition temperature was modeled by the form[36]

$$T_{\mathrm{g}}^{\mathrm{A}}(\phi^{\mathrm{A}}_{\text{eff}}) = \frac{T_{\mathrm{gA}}\phi^{\mathrm{A}}_{\text{eff}} + T_{\mathrm{gB}}(1 - \phi^{\mathrm{A}}_{\text{eff}})Q}{\phi^{\mathrm{A}}_{\text{eff}} + (1 - \phi^{\mathrm{A}}_{\text{eff}})Q} \tag{17a}$$

where T_{gA} and T_{gB} are the glass transition temperatures for pure A and B components, respectively. If $Q = T_{\mathrm{gA}}/T_{\mathrm{gB}}$, then eq 17a reduces to the well-known Fox equation:[37,38]

$$\frac{1}{T_{\mathrm{g}}^{\mathrm{A}}(\phi^{\mathrm{A}}_{\text{eff}})} = \frac{\phi^{\mathrm{A}}_{\text{eff}}}{T_{\mathrm{gA}}} + \frac{1 - \phi^{\mathrm{A}}_{\text{eff}}}{T_{\mathrm{gB}}} \tag{17b}$$

If, on the other hand, Q were assigned as a fit parameter, then eq 17a is nothing but the DiMarzio form. To be consistent with the preceding paper, we shall use the Fox equation for our calculations of local dynamics, although as we shall discuss below, the DiMarzio form performs comparably in the prediction of blend dynamics. The values of glass transition temperatures of pure components are listed in Table 1. Figure 1 plots the composition dependence of T_g for the four blends we consider in this paper. The dotted lines are the Fox equation (eq 17b), the thin solid lines are the fits of the DiMarzio equation (eq 17a with Q as a fit parameter), and the thick solid lines are the outcome of our model, to be discussed below.

We use the respective pure component values for C_1 and τ_g even in the mixtures, to emphasize that the local dynamics of the materials (i.e., torsion angle flips) are probably unaffected by blending. The C_2 parameter in the blend is assumed to

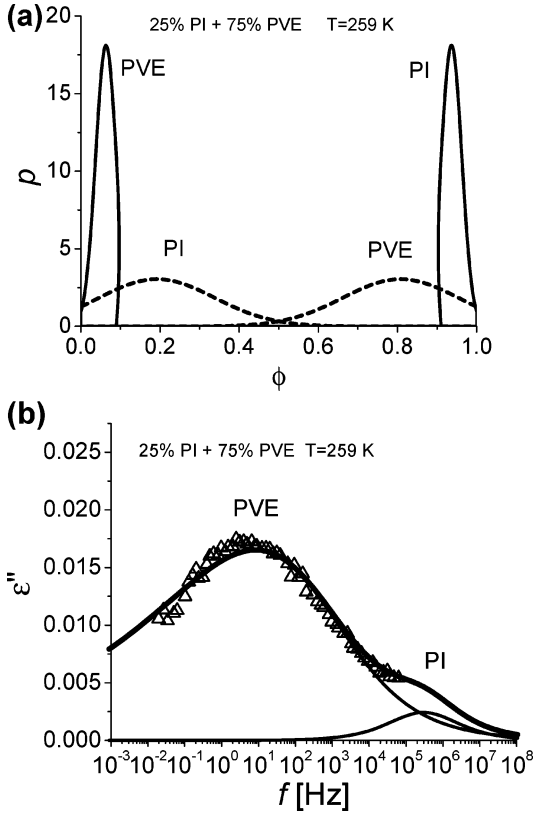

Figure 2. (a) PDFs for local volume fraction of each component in a 25% PI + 75% PVE blend at $T = 259$ K, calculated for volumes with $R_c = 3.7$ Å, centered around PI segments (the PI distribution is the right solid curve and the PVE distribution is the left solid curve) and for volumes with $R_c = 9.0$ Å, centered around PVE segments (the PVE distribution is the right dashed curve and the PI distribution is the left dashed curve). (b) Frequency dependence of dielectric loss at $T = 259$ K, calculated from these distributions (thick line), obtained as the sum of the separate contributions from PI and PVE relaxations (thin lines) and experimental data taken from ref 9 (points).

have a linear composition dependence:

$$C_2^{\mathrm{A}} = C_{2\mathrm{A}}\phi_{\mathrm{eff}}^{\mathrm{A}} + C_{2\mathrm{B}}(1 - \phi_{\mathrm{eff}}^{\mathrm{A}}) \tag{18}$$

where $C_{2\mathrm{A}}$ and $C_{2\mathrm{B}}$ are parameter values for pure A and B components. We have also used composition independent values of C_2 but find practically identical results.

Equations 15−18 will convert the Gaussian distribution function for ϕ_{eff} (eq 5) to an asymmetric distribution function for log τ, with the maximum shifted from the value corresponding to the mean composition $\bar{\phi}_{\mathrm{eff}}$.[23] Therefore, the actual frequency of the dielectric loss peak is defined not only by the mean composition $\bar{\phi}_{\mathrm{eff}}$ but also by the width of the composition distribution function $\langle \delta\phi_{\mathrm{eff}}^2 \rangle$.

The dielectric loss peak of each component can be calculated assuming some relaxation form of each individual process, such as the Debye form, and the PDF for the segmental relaxation times, $p_\tau(\ln \tau)$ (eq 15):

$$\epsilon_{\mathrm{A}}^{||}(\omega) = I_{\mathrm{A}}\Phi_{\mathrm{A}}\int_{-\infty}^{+\infty} p_\tau(\ln \tau)\frac{\omega\tau}{1 + (\omega\tau)^2}\, \mathrm{d} \ln \tau \tag{19}$$

where $\omega = 2\pi f$ is the frequency and I_{A} is the specific peak magnitude, proportional to the polarizability of the component. However, relaxation peaks predicted from eq 19 are usually too narrow[27] since no density fluctuations are included. To account for the additional broadening and asymmetry of each relaxation process resulting from density fluctuations, the Debye function was replaced with its empirical modification—the Havriliak−Negami function:[27]

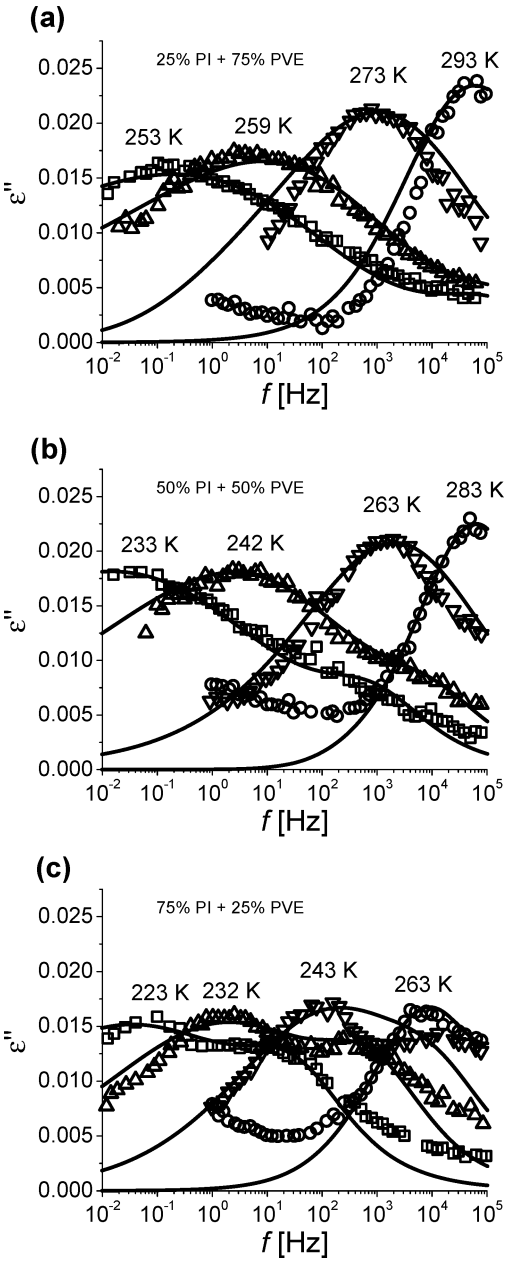

Figure 3. Frequency dependence of dielectric loss at various temperatures for blends composed by weight percent of (a) 25% PI + 75% PVE, (b) 50% PI + 50% PVE, and (c) 75% PI + 25% PVE. Experimental data (points) are taken from ref 9. Solid lines show model predictions with nonadjustable parameters summarized in Table 1; R_c(PI) and R_c(PVE) values are plotted in Figure 6a,b.

$$\epsilon_{\mathrm{A}}^{||}(\omega) = I_{\mathrm{A}}\Phi_{\mathrm{A}}\int_{-\infty}^{+\infty} p_\tau(\ln \tau)\left[1 + (\omega\tau_{\mathrm{HN}})^{2\alpha} + 2(\omega\tau_{\mathrm{HN}})^{\alpha} \cos\left(\frac{\pi\alpha}{2}\right)\right]^{-\gamma/2} \sin\left(\gamma \tan^{-1}\left[\frac{\sin(\pi\alpha/2)}{(\omega\tau_{\mathrm{HN}})^{-\alpha} + \cos(\pi\alpha/2)}\right]\right) \mathrm{d} \ln \tau;$$

$$\tau_{\mathrm{HN}} = \tau\left[\tan\left(\frac{\pi}{2(\gamma + 1)}\right)\right]^{1/\alpha} \tag{20}$$

The parameters α and γ were calculated from the fits to the experimental relaxation data for pure components (Table 1).[27]

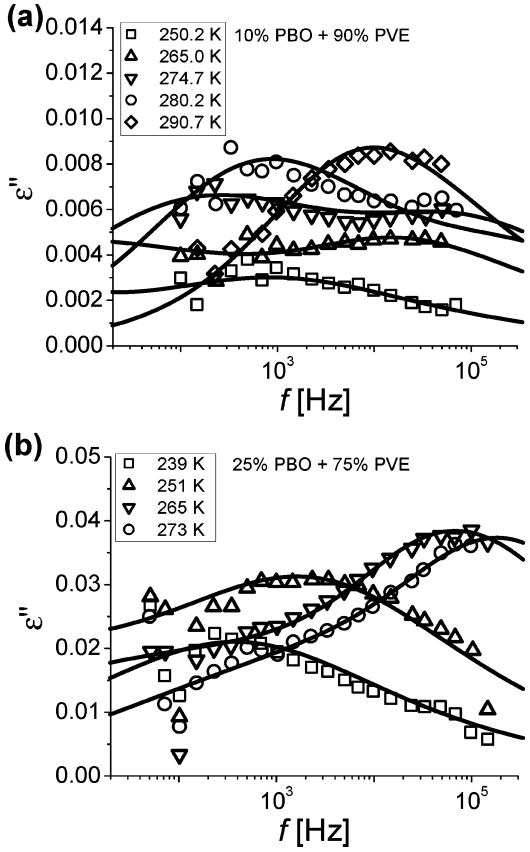

Figure 4. Frequency dependence of dielectric loss at various temperatures for blends composed by weight percent of (a) 10% PBO + 75% PVE and (b) 25% PBO + 75% PVE. Experimental data (points) are taken from ref 39. Solid lines show model predictions with nonadjustable parameters summarized in Table 1; R_c(PI) and R_c(PVE) values are plotted in Figure 6a,b.

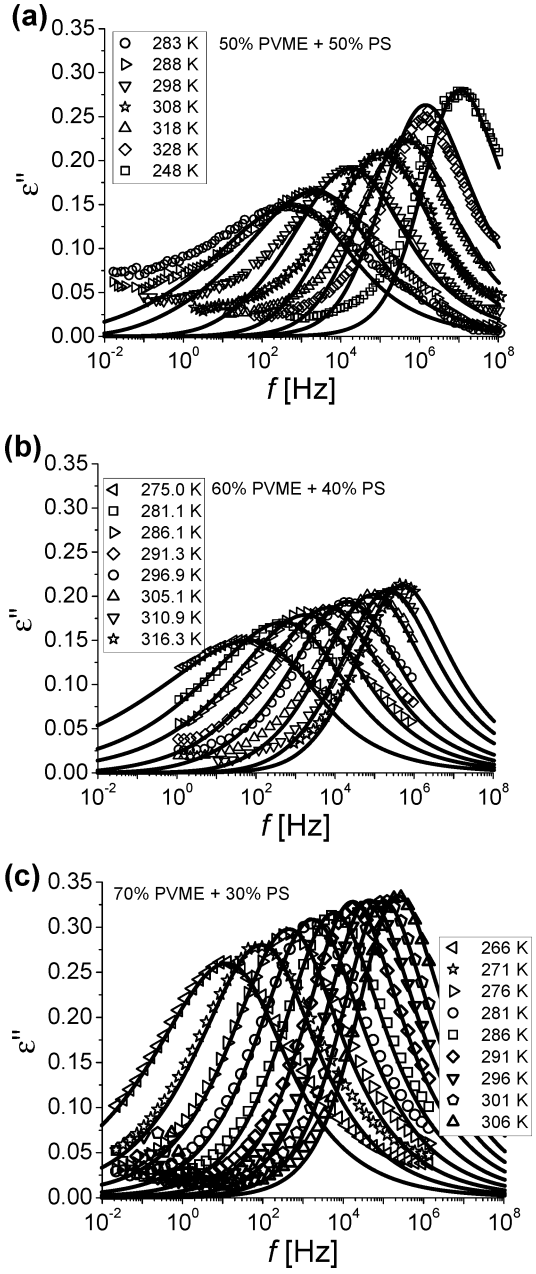

Figure 5. Points: frequency dependence of dielectric losses at various temperatures for blends composed by weight percent of (a) 50% PVME + 50% PS (ref 43), (b) 60% PVME + 40% PS (ref 44), and (c) 70% PVME + 30% PS (ref 45). Solid lines: model predictions for PVME relaxation with parameters summarized in Table 1 and R_c values plotted in Figure 8a.

3. Comparing Model Predictions with Experiments

We analyzed dielectric relaxation data for four different polymer blends: 1,4-polyisoprene/poly(vinylethylene) (PI/PVE), poly(butylene oxide)/poly(vinylethylene) (PBO/PVE), polystyrene/poly(vinyl methyl ether) (PS/PVME), and poly(2-chlorostyrene)/poly(vinyl methyl ether) (P2ClS/PVME) with various compositions. The experimentally defined parameters used to generate the predictions are summarized in Table 1. Dielectric relaxation peaks were fitted individually for each component according to eqs 5, 6, 12, 13, 15, 16, 17b, 18, and 20 using conjugate gradient least-squared deviation procedure with the size of correlation volume R_c and normalization I as parameters. The variation of correlation radius R_c simultaneously affects the position, shape, and the width of the relaxation peak, while the variation of I only affects the magnitude of the dielectric loss. This allows us to extract both fitting parameters independently from well-defined experimental relaxation peaks.

Figure 2a shows the PDFs for local composition in a 25% PI/75% PVE blend, calculated for spherical volumes with radius $R_c = 3.7$ Å, for PI while it is $R_c = 9.0$ Å for PVE. (For comparison, similar results were obtained for the DiMarzio model but using $R_c = 5.90$ Å for PI and $R_c = 5.35$ Å for PVE segments.) The abrupt cutoffs in the Gaussian distributions are at ϕ_{self} (~0.9 for PI and 0.65 for PVE). The figure clearly demonstrates that these composition distributions are different depending on the volume positioning, but symmetric for two components within the same volumes. Figure 2b compares the predicted dielectric response of PI, PVE, and their sum with experimental data on the same 25/75 blend at 259 K. The predictions compare quite favorably with the experimental measurements.

Figures 3−5 present our results for fits to the dielectric loss for three different blends, while Figures 6 and 8 report the R_c values used in each case. Figure 3a−c compares the predicted sum dielectric loss distribution for PI/PVE blends (solid curves) at various temperatures with dielectric spectroscopy experimental data[9] (points). The width of the concentration distribution function that ultimately leads to the solid lines in Figure 3 was calculated using eq 12. As temperature decreases, the peak position in each case moves toward longer relaxation times and the distributions broaden. The theory captures all these features of the experimental data with fidelity. Furthermore, for the whole studied temperature interval, the model predicts remarkably correct peak widths in both PVE-rich and PI-rich compositions

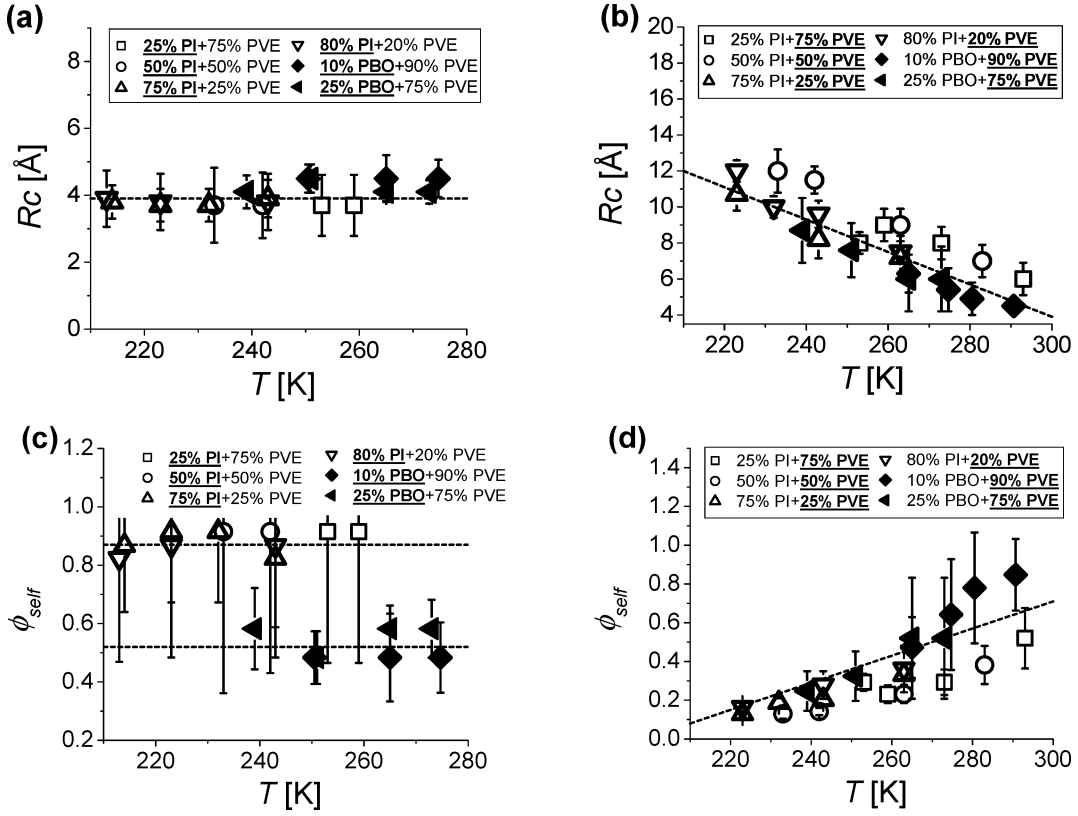

Figure 6. (a, b) Temperature dependence of correlation radius R_c for dielectric relaxation of each component in PI/PVE and PBO/PVE blends with compositions shown in the legend (relevant component is denoted in bold). (c, d) Corresponding plots of self-concentrations calculated using eq 2. The lines are guides to the eye.

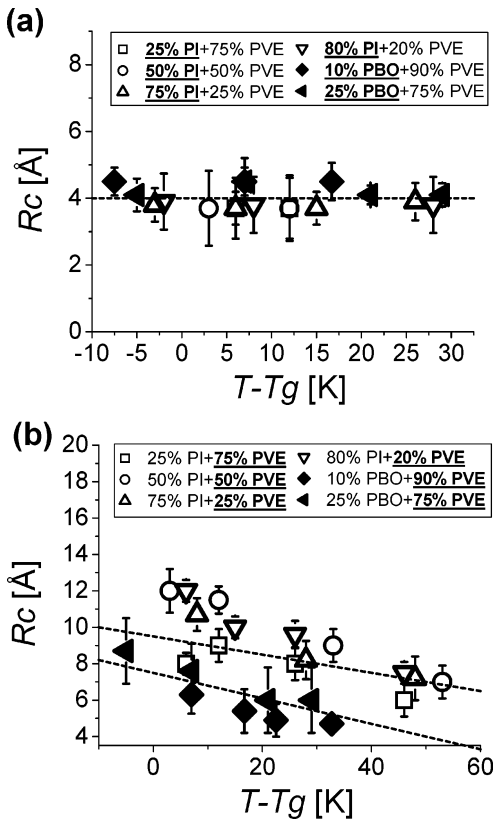

Figure 7. Data from Figure 6a,b plotted against $T - T_g$, where T_g is the glass transition temperature of the blend.

in the range 25−75%. Two compositions of PBO/PVE blends[23] are treated similarly in Figure 4a,b, at various temperatures, with similar conclusions.

In PVME/PS blends (Figure 5a−c), only the PVME component contributes to the dielectric relaxation, giving us a possibility to compare the shape of the relaxation peak with model predictions. The correlation radius for PVME relaxation R_c(PVME) is the only parameter which affects simultaneously the position, width, and asymmetric shape of the peak. As can be concluded from Figure 5, the model predictions are remarkably accurate. The overall agreement with experiment is very good for all temperatures and compositions, providing strong evidence that local composition fluctuations are the key factor for understanding the broadening of dielectric loss on blending.

The normalization parameter I for PVME relaxation (numerically equal to the area of the calculated dielectric loss peak in log(f) coordinates divided by volume fraction of PVME component) is plotted in Figure 9. The area of the peaks decreases with temperature in a usual fashion related to density change by the Clausius−Mosotti equation[11] with specific polarizability 0.89 cm^3/g (solid curves).

The temperature dependences of the correlation radius R_c for all components in PI/PVE and PBO/PVE blends and for PVME relaxation in PVME/PS blends are plotted in Figures 6 and 8. The error bars were calculated from both the standard deviation of the parameters R_c from the "best fit" value and the typical accuracy of dielectric relaxation experiments. In contrast to the results of our previous studies,[22] the values of R_c collapse onto a single curve for various blend compositions, thus suggesting no composition dependence of the correlation radius. (Figure 7 plots the data in Figure 6 against $T - T_g$rather than against T. Clearly, this is an inferior representation than Figure 6.) We attribute this change to the more accurate evaluation of fluctuations utilized here for intramolecular distributions of concentrations. The radius of the correlation volume is of the order of 4 Å (PI and PBO), 4−10 Å (PVE), and 5−6 Å

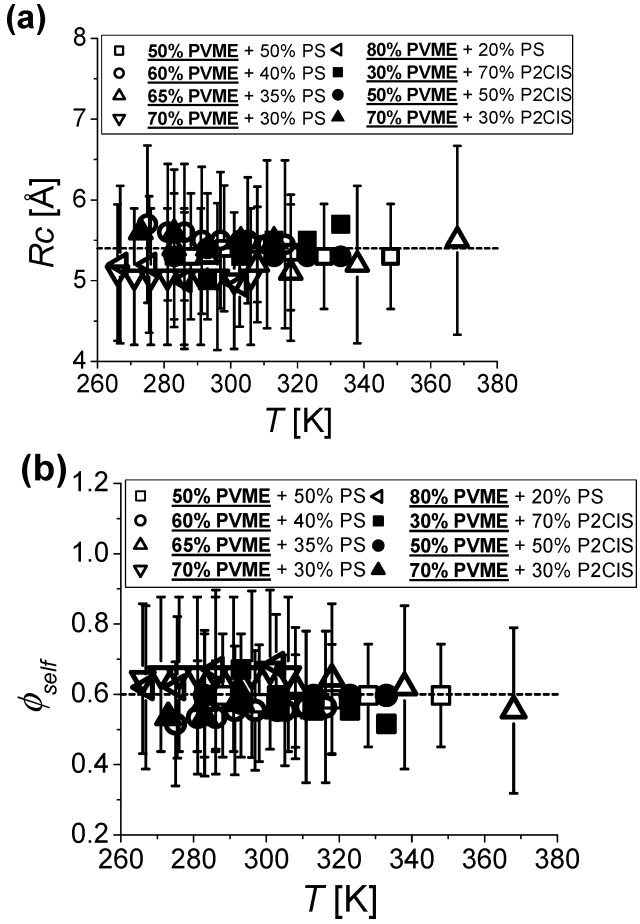

Figure 8. (a) Temperature dependence of correlation radius R_c for dielectric relaxation of PVME in PVME/PS and PVME/P2ClS blends with compositions shown in the legend. (b) Corresponding plots of self-concentrations derived using eq 2. The lines are the guides to the eye.

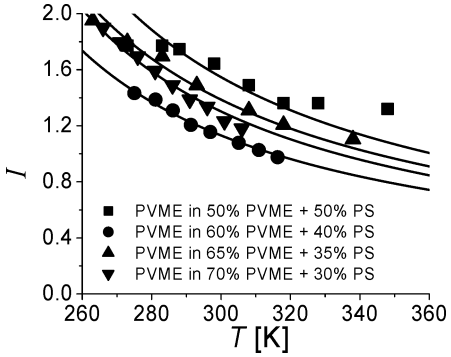

Figure 9. Normalization parameter I used to fit dielectric relaxation data for PVME/PS blends shown in Figure 5 (points) and the decrease of peak area predicted from density change using the Clausius−Mosotti equation with specific polarizability $A = 0.89$ cm^3/g (lines).

(PVME). [In contrast, the DiMarzio model yielded ∼4 Å (PI and PBO), 5−7 Å (PVE), and 8−10 Å (PVME).] These numbers do not exceed the Kuhn length of each polymer, thus validating the assumption made for calculation of the intramolecular concentration distribution (eq 2). The values defined here for R_c(PVE) are close to the assumptions made by Lodge and McLeish[21] for their model and to values obtained in our earlier model.[22] Furthermore, Figure 6a shows only a moderate increase of the size of the correlation volume for the PVE component with decreasing temperature (solid points), while for PVME, PI, and PBO components no temperature dependence of R_c was found. The respective self-concentrations, calculated using eq 2, are plotted in Figures 6 and 7. The trends for PVE shown in Figure 6d resemble the results of our previous model,[22] with the essential difference that no composition dependence and only a weak temperature dependence were found in the improved model.

Table 2. Average Values of Correlation Radius and Respective Values of Self-Concentration, Found from the Fits of Eq 20 to the Dielectric Relaxation Data[a]

components	R_c (Å)	ϕ_{self}	T_g (K)
PI	4	0.78	210
PVE	8	0.29	273
PBO	4.3	0.51	200
PVE-89	8	0.29	269
PVME	5.4	0.57	249
PS	∼25	0.053	379
P2ClS	16	0.13	402

[a] Value for PS was found from best fit to the DSC data shown in Figure 1c. Last column shows the T_g values of the components.

The next question of interest is whether R_c is a polymer-specific property or a blend property that depends on blend partner. The results for the PVE and PVME blended with two different partners each are also presented in Figures 6 and 8. It is clear that, within the uncertainties, the size of the correlation volume is independent of the partner. This conclusion is consistent with our previous statement that the correlation radius is independent of blend composition and that the correlation radius is small and comparable with the Kuhn length. Moreover, no signature of blend glass transition was found in the temperature dependence of R_c. For example, the T_g of PVME/PS 50/50 blend is 280 K, and the $R_c(T)$ dependence for the PVME component does not change abruptly in the vicinity of this temperature. The averaged constant values of correlation radii and respective self-concentrations are summarized in Table 2. R_c increases smoothly with T_g.

4. Discussion

We first focus on the fact that the Fox equation provides such good fits to experimental data, even though it apparently only provides a poor prediction of the DSC determined T_g values for the different blends (Figure 1). To resolve this apparent discrepancy, we follow a procedure suggested by Lodge and McLeish and assume that the Fox equation adequately describes the glass transition in a volume of R_c for each component. We now model the global (DSC) glass transition as a superposition of the relaxations of the two components:

$$\langle T_g \rangle = \langle T_g^A \rangle \Phi_A + \langle T_g^B \rangle \Phi_B \tag{21}$$

Assuming $\langle T_g^A \rangle = T_g(\langle \phi_{eff}^A \rangle)$, the Fox equation (eq 17b) gives $\langle T_g^A \rangle = T_{gA} T_{gB} / (T_{gA} + \Delta T_g \phi_{eff}^A)$, where $\Delta T_g \equiv T_{gB} - T_{gA}$. Some simplification then allows us to reduce eq 21 to

$$\langle T_g \rangle = \frac{T_{gA} T_{gB} [T_{gA} \Phi_B + T_{gB} \Phi_A + \Delta T_g (\Phi_B^2 \phi_{self}^A - \Phi_A^2 \phi_{self}^B)]}{[T_{gA} + \Delta T_g \Phi_A (1 - \phi_{self}^B)][T_{gB} - \Delta T_g \Phi_B (1 - \phi_{self}^A)]} \tag{22}$$

Employing the self-concentration for the two species then permits the calculation represented in eq 22. (In the case of PS, which is dielectrically inactive, we assumed $R_c = 25$ Å which best fit the DSC data.) The thick lines in Figure 1 which represent the results from this approach satisfactorily model the experimental results, providing some basis for why the Fox equation is adequate to model blend dynamics.

A second issue we wish to reemphasize is the robustness of our procedure to chosen forms for describing the composition dependence of T_g, i.e., the Fox vs the DiMarzio forms. As we have reported throughout, we can obtain adequate fits to experimental data but with R_c values which can be quite different depending on which model is employed. Since no systematic trend is found for these correlation radii, we suggest that, while they appear to be small and independent of blend composition and partner, their absolute numbers are too dependent on the modeling procedure for these quantities to have any molecular significance. Without a reliable model for the glass transition, we are therefore forced to use R_c merely as a fitting parameter but with some relatively stringent constraints, i.e., that it be of order the Kuhn length and be independent of the blend partner and composition.

5. Summary and Conclusions

We have developed a theoretical model to comprehensively understand the dynamics of miscible, weakly interacting polymer blends. This is achieved by modeling the distribution function of the effective concentration around a test segment in terms of intrachain and interchain contributions. The effective blend composition distribution for each species is transformed into the distribution function for the glass transition temperature and then into the distribution function for segmental relaxation times using standard methods. The only quantity that remains unspecified in this approach is the size of the correlation volume over which fluctuations have to be sampled, and we determine this quantity by fitting our model to a large body of data on miscible PI/PVE, PBO/PVE, PVME/PS, and PVME/P2ClS blends, with the correlation radius R_c and the dielectric strength as the only fitting parameters.

In contrast to our past work,[22] which had required this correlation volume to be a strong function of both temperature and blend composition, we find that a *composition-independent* correlation volume is sufficient to quantitatively model experimental data, independent of blend partner and with only a weak temperature dependence. The diameter of the spherical correlation volume is comparable to the Kuhn length of the chains, in good agreement with Lodge and McLeish.[21] The weak temperature dependence of R_c might well be due to the assumptions we make regarding the connection between composition and relaxation time or could reflect weak temperature dependence of either the Kuhn or packing lengths.

In the model introduced by Zetsche and Fischer,[17] larger correlation volumes were needed to describe the experimental distribution width. This is because they essentially assumed $\langle\delta\phi^2\rangle \propto S(0)/R_c^3$, whereas we derive $\langle\delta\phi^2\rangle \propto S(0)/(\xi^2 R_c)$ (see eq 14). Since $\xi > R_c$, our new model gives the fluctuations needed to describe data using a considerably smaller correlation volume. In our model, we carefully calculated a Gaussian approximation to the concentration distribution, with the assumption that local composition fluctuations dominate local density variations (incompressible blend approximation). In reality, density fluctuations are expected to be important, and incorporating those effects would allow the use of somewhat larger correlation volumes.

Our model has shown that, with a correlation volume diameter comparable to the Kuhn length, the fluctuations of local composition reasonably predict the width of the relaxation spectra over broad ranges of temperature and blend composition. Furthermore, the position of the relaxation peak is strongly affected by the fluctuations of local composition,[38] particularly near T_g. In order to quantitatively capture all aspects of blend dynamics, including the width and the position of the relaxation time distributions, it is vital to include concentration fluctuations effects.

Acknowledgment. We are grateful for the financial support from the National Science Foundation (DMR-0422079).

References and Notes

(1) Ferry, J. D. *Viscoelastic Properties of Polymers*, 3rd ed.; Wiley: NewYork, 1980.
(2) Brosseau, C.; Guillermo, A.; Cohen-Addad, J. P. *Macromolecules* **1992**, *25*, 4535.
(3) Waestlund, C.; Maurer, F. H. J. *Macromolecules* **1997**, *30*, 5870.
(4) Ngai, K. L.; Roland, C. M. *Macromolecules* **2004**, *37*, 2817.
(5) Prest, W. M.; Porter, R. S. *J. Polym. Sci., Part A-2: Polym. Phys.* **1972**, *10*, 1639.
(6) Colby, R. H. *Polymer* **1989**, *30*, 1275.
(7) Chung, G.-C.; Kornfield, J. A.; Smith, S. D. *Macromolecules* **1994**, *27*, 964.
(8) Chung, G.-C.; Kornfield, J. A.; Smith, S. D. *Macromolecules* **1994**, *27*, 5729.
(9) Alegria, A.; Colmenero, J.; Ngai, K. L.; Roland, C. M. *Macromolecules* **1994**, *27*, 4486.
(10) Alvarez, F.; Alegria, A.; Colmenero, J. *Macromolecules* **1997**, *30*, 597.
(11) Pathak, J. A.; Colby, R. H.; Floudas, G.; Jerome, R. *Macromolecules* **1999**, *32*, 2553.
(12) Tomlin, D. W.; Roland, C. M. *Macromolecules* **1992**, *25*, 2994.
(13) Pathak, J. A.; Colby, R. H.; Kamath, S. Y.; Kumar, S. K.; Stadler, R. *Macromolecules* **1998**, *31*, 8988.
(14) Alegria, A.; Elizetxea, C.; Cendoya, I.; Colmenero, J. *Macromolecules* **1995**, *28*, 8819.
(15) Friedrich, C.; Schwarzwaelder, C.; Riemann, R. E. *Polymer* **1996**, *37*, 2499.
(16) Pathak, J. A.; Colby, R. H.; Kumar, S. K.; Krishnamoorti, R. *Proceedings of the XIIIth International Congress on Rheology*, Cambridge, I-257, 2000.
(17) Zetsche, A.; Fischer, E. W. *Acta Polym.* **1994**, *45*, 168.
(18) Katana, G.; Fischer, E. W.; Hack, T.; Abetz, V.; Kremer, F. *Macromolecules* **1995**, *28*, 2714.
(19) Donth, E. J. *Relaxation and Thermodynamics in Polymers*; Akademie Verlag: Berlin, 1992.
(20) Reference deleted in proof.
(21) Lodge, T. P.; McLeish, T. C. B. *Macromolecules* **2000**, *33*, 5278.
(22) Kant, R.; Kumar, S. K.; Colby, R. H. *Macromolecules* **2003**, *36*, 10087.
(23) Kumar, S. K.; Shenogin, S.; Colby, R. H. *Macromolecules* **2007**, *40*, 5759.
(24) Lutz, T. R.; He, Y.; Ediger, M. D.; Pitsikalis, M.; Hadjichristidis, N. *Macromolecules* **2004**, *37*, 6440.
(25) Kumar, S. K.; Colby, R. H.; Anastasiadis, S. H.; Fytas, G. *J. Chem. Phys.* **1996**, *105*, 3777.
(26) Kamath, S.; Colby, R. H.; Kumar, S. K.; Karatasos, K.; Floudas, G.; Fytas, G.; Roovers, J. E. L. *J. Chem. Phys.* **1999**, *111*, 6121.
(27) Colby, R. H.; Lipson, J. E. G. *Macromolecules* **2005**, *38*, 4919.
(28) Song, H. H.; Roe, R. J. *Macromolecules* **1987**, *20*, 2723.
(29) Salaniwal, S.; Kant, R.; Colby, R. H.; Kumar, S. K. *Macromolecules* **2002**, *35*, 9211.
(30) Higgins, J. S.; Benoit, H. C. *Polymers and Neutron Scattering*; Oxford University Press: New York, 1994.
(31) Fetters, L. J.; Lohse, D. J.; Graessley, W. W. *J. Polym. Sci., Part B:* **1999**, *37*, 1023.
(32) de Gennes, P.-G. *Scaling Concepts in Polymer Physics*; Cornell University Press: Ithaca, NY, 1979.
(33) Tomlin, D. W.; Roland, C. M. *Macromolecules* **1992**, *25*, 2994.
(34) Krishnamoorti, R.; Graessley, W. W.; Fetters, L. J.; Garner, R. T.; Lohse, D. J. *Macromolecules* **1995**, *28*, 1252.
(35) Rubinstein, M.; Colby, R. H. *Polymer Physics*; Oxford University Press: New York, 2003.
(36) DiMarzio, E. A. *Polymer* **1990**, *31*, 2294.
(37) Schneider, H. A. *J. Res. Natl. Inst. Stand. Technol.* **1997**, *102*, 229.
(38) Fox, T. G. *Bull. Am. Phys. Soc.* **1956**, *2*, 123.
(39) Hirose, Y.; Adachi, K. *Macromolecules* **2006**, *39*, 1779.
(40) Urakawa, O.; Fuse, Y.; Hori, H.; Tran-Cong, Q.; Yano, O. *Polymer* **2001**, *42*, 765.
(41) Hirose, Y.; Urakawa, O.; Adachi, K. *Macromolecules* **2003**, *36*, 3699.
(42) Lorthioir, C.; Alegría, A.; Colmenero, J. *Phys. Rev. E* **2003**, *68*, 03805.
(43) Leroy, E.; Alegría, A.; Colmenero, J. *Macromolecules* **2003**, *36*, 7280.
(44) Zetsche, A.; Kremer, F.; Schulze, W. J.-H. *Polymer* **1990**, *31*, 1883.
(45) Pathak, J. A. Miscible Polymer Blends Dynamics. Doctoral Dissertation, The Pennsylvania State University, University Park, PA, 2001.

MA070503Q